Title
The C-Terminal Repeating Units of CsgB Direct Bacterial Functional Amyloid Nucleation

Journal
Journal of Molecular Biology, 422(3)

ISSN
0022-2836

Authors
Hammer, Neal D
McGuffie, Bryan A
Zhou, Yizhou
et al.

Publication Date
2012-09-01

DOI
10.1016/j.jmb.2012.05.043

Peer reviewed

Published in final edited form as:
J Mol Biol. 2012 September 21; 422(3): 376–389. doi:10.1016/j.jmb.2012.05.043.

The C-terminal repeating units of CsgB direct bacterial functional amyloid nucleation

Neal D. Hammer[1], **Bryan A. McGuffie**[‡], **Yizhou Zhou**[‡], **Matthew P. Badtke**[‡], **Ashley A. Reinke**[¥], **Kristoffer Brännström**[€], **Jason E. Gestwicki**[¥], **Anders Olofsson**[€], **Fredrik Almqvist**[§,†], and **Matthew R. Chapman**[€,‡,*]

[1]Department of Microbiology and Immunology, University of Michigan Medical School, Ann Arbor, MI 48109-0620 U.S.A

[¥]Life Sciences Institute, University of Michigan, Ann Arbor, MI 48109 U.S.A

[€]Medical Biochemistry and Biophysics, Chemical Biological Center, Umeå University, 901 87 Umeå, Sweden

[§]Department of Chemistry, Chemical Biological Center, Umeå University, 901 87 Umeå, Sweden

[†]Umeå Center for Microbial Research, Umeå University, 901 87 Umeå, Sweden

[‡]Department of Molecular, Cellular, and Developmental Biology, University of Michigan LSA,830 North University, Ann Arbor, MI 48109 U.S.A

Abstract

Curli are functional amyloids produced by enteric bacteria. The major curli fiber subunit, CsgA, self-assembles into an amyloid fiber *in vitro*. The minor curli subunit protein, CsgB, is required for CsgA polymerization on the cell surface. Both CsgA and CsgB are composed of five predicted β–strand-loop-β–strand-loop repeating units that feature conserved glutamine and asparagine residues. Because of this structural homology, we proposed that CsgB might form an amyloid template that initiates CsgA polymerization on the cell surface. To test this model, we purified wild-type CsgB, and found that it self-assembled into amyloid fibers *in vitro*. Preformed CsgB fibers seeded CsgA polymerization as did soluble CsgB added to the surface of cells secreting soluble CsgA. To define the molecular basis of CsgB nucleation, we generated a series of mutants that removed each of the five repeating units. Each of these CsgB deletion mutants was capable of self-assembly *in vitro. In vivo*, membrane-localized mutants lacking the 1st, 2nd or 3rd repeating units were able to convert CsgA into fibers. However, mutants missing either the 4th or 5th repeating units were unable to complement a *csgB* mutant. These mutant proteins were not localized to the outer membrane, but were instead secreted into the extracellular milieu. Synthetic CsgB peptides corresponding to repeating units 1, 2 and 4 self assembled into ordered amyloid polymers, while peptides corresponding to repeating units 3 and 5 did not, suggesting that there are redundant amyloidogenic domains in CsgB. Our results suggest a model where the rapid conversion of CsgB from unstructured protein to a β-sheet-rich amyloid template anchored to the cell surface is mediated by the C-terminal repeating units.

[*]To whom correspondence should be addressed: Matthew R. Chapman, Department of Molecular, Cellular, and Developmental Biology, University of Michigan LSA, 830 North University, Ann Arbor, MI 48109 USA, Tel.: (734)764-7592; Fax: (734)647-0884; chapmanm@umich.edu.

Introduction

Amyloid fibers are a common pathology associated with neurodegenerative diseases such as Alzheimer's and Parkinson's disease [1]. These have classically been referred to as protein misfolding diseases because the amyloidogenesis is the result of an aberrant aggregation process in which a normally soluble protein self assembles into a highly ordered, structurally stable fiber. Biochemically, amyloid fibers are defined by unique tinctorial properties, resistance to proteases and detergents and a β-sheet rich secondary structure [2]. Typically there are three phases to *in vitro* amyloid polymerization: a lag phase, a phase of rapid fiber growth and a stationary phase [3; 4; 5; 6; 7; 8]. Rapid fiber growth is dependent on the formation of a nucleus [9]. A common feature of nucleus-dependent polymerization reactions is that preformed fibers can act to seed the polymerization of soluble monomers. It is proposed that preformed fibers provide a template for monomer polymerization, and that this interaction mediates exit from the lag phase [9]. Although amyloid nucleation and polymerization have been extensively studied *in vitro*, *in vivo* nucleation models are just now being developed. Functional amyloids provide a robust context to study *in vivo* amyloid nucleation and polymerization, especially in cases where the functional amyloid is produced by a genetically tractable model organism [10; 11; 12].

Curli fibers are extracellular amyloid fibers produced by *E. coli* and other enteric bacteria [10; 13]. The discovery of a dedicated pathway for amyloid biogenesis in curli fiber assembly led to a paradigm shift in the amyloid field, which previously held that amyloids were exclusively the result of protein misfolding. Curli fibers are part of the extracellular matrix that is required for biofilm formation and for mediating host cell-bacteria interactions [14; 15; 16; 17; 18]. Therefore, curli are virulence factors [19; 20; 21] and constitute potential novel targets for antibacterial agents [22; 23; 24]. Curli are composed of a major and minor subunit, CsgA and CsgB, respectively [25; 26; 27]. Purified CsgA polymerizes into an amyloid fiber *in vitro*, but CsgB is required for *in vivo* curli formation [8; 28]. In the absence of CsgB, CsgA is secreted away from the cell as a soluble protein [26; 29]. In a process referred to as interbacterial complementation, cell surface localized CsgB produced by a *csgA* mutant can convert secreted, soluble CsgA produced by a *csgB* mutant into an ordered amyloid fiber [10; 28]. The CsgB expressed on the surface of *csgA* mutants can also nucleate exogenously added purified CsgA [30; 31]. CsgB becomes incorporated into the fiber after initiating the polymerization of CsgA [25], yet the sequences or domains of CsgB that guide amyloid nucleation have yet to be elucidated.

In silico structural predictions suggest that both CsgA and CsgB contain a β-sheet rich domain that can be further divided into five imperfect β-strand-loop-β-strand repeats [26; 32; 33]. The repeating unit domains of both CsgA and CsgB are 51% similar and they contain a number of conserved glutamines and asparagines [27]. These observations led us to hypothesize that CsgB, like CsgA, may also adopt an amyloid-like fold and that this feature of CsgB may serve to template CsgA polymerization. We previously purified a truncated version of CsgB missing the fifth repeating unit ($CsgB^{\Delta r5}$) [34]. This truncated CsgB mutant self-assembled into β-sheet rich amyloid fibers that could template CsgA polymerization *in vitro*. However, unlike WT CsgB, CsgB missing the fifth repeating unit was secreted away from the cell surface and was unable to complement a *csgB* mutant *in vivo* [34].

We report here that wild-type (WT) CsgB polymerizes into an amyloid structure and does so faster than either CsgA or the previously characterized CsgB truncation mutant. Purified WT CsgB was able to template CsgA polymerization *in vitro* and *in vivo* when applied to *csgB* mutants. The contribution of each CsgB repeating unit to nucleator function *in vivo* and to CsgB polymerization *in vitro* was assessed. We found that the fourth repeating unit of CsgB

is required for cell association suggesting that both the 4th and 5th repeating units function, directly or indirectly, to anchor CsgB to the cell. Our results support a model in which CsgB rapidly adopts a β-sheet-rich, amyloid fold at the cell surface that templates the conversion of slower-folding major subunit CsgA into cell-associated amyloid fibers. We propose that this process is mediated by the C-terminal repeating units of CsgB.

Results

Purified CsgB forms amyloid fibers that can seed CsgA polymerization

CsgB contains three domains. The first domain contains twenty-one amino acids and encodes a *sec*-signal sequence responsible for targeting CsgB to the periplasm. These amino acids are cleaved as the protein transverses the inner-membrane. The next twenty-two amino acids mark the N-terminus of the mature protein. This domain is predicted to be unstructured and cells expressing CsgB deleted for these amino acids produce WT fibers (data not shown). However, the synonymous region within CsgA is required for the secretion of the protein [35; 36]. The last domain contains the amyloid-core of CsgB and can be further divided into five regions of imperfect homology referred to as repeating units. We previously purified a truncated CsgB molecule that lacked the C-terminal repeating unit by harvesting the supernatant of cells expressing the truncated protein. Attempts to purify WT CsgB from the extracellular milieu in a similar fashion were impeded by relatively low expression levels [34]. Here, expression of mature WT CsgB (i.e. the WT sequence of CsgB lacking only the *sec*-signal sequence required for secretion across the inner membrane) was induced in the cytoplasm of cells. After induction, cells contained significant amounts of SDS insoluble CsgB protein (Fig. 1A lane 2 and 3). Soluble his-tagged CsgB was recovered by affinity purification after pellets of induced cells were resuspended in 8 M GndHCl (Fig. 1A lane 4) [33].

CsgB polymerization was monitored over time using the amyloid specific dye thioflavin-T (ThT). ThT fluorescence rapidly increased upon addition of freshly purified, soluble CsgB after only a short lag phase, and this increase in fluorescence was concentration dependent (Fig. 1B). Both CsgA and CsgB polymerization curves contained a lag phase, a fast phase, and a stationary phase. However, the CsgB lag phase was shorter than the CsgA lag phase at approximately equivalent protein concentrations (Fig. 1B). Transmission electron microscopy (TEM) analysis of fractions containing CsgB incubated overnight at room temperature revealed an ordered fibrous structure, similar to what has been observed for CsgA (Fig. 1C) [8]. The fibrous CsgB aggregates were not soluble in SDS and pretreatment with formic acid (FA) was required to visualize monomeric protein on a SDS-PAGE gel (Fig. 1D lane 2).

To test whether CsgB fibers could template CsgA polymerization *in vitro*, we measured the polymerization of soluble CsgA in the presence of preformed CsgB fibers by ThT fluorescence. In the absence of CsgB, CsgA polymerization had a lag phase of approximately two hours. When 5% (w/w) preformed CsgB fibers were added to the reaction mix, a 1-hour lag phase was observed. When the amount of CsgB fibers was increased to 12% (w/w), CsgA polymerization proceeded without an apparent lag phase at this time scale (Fig. 1E). Interaction of soluble CsgA with CsgB fibers was also monitored by surface plasmon resonance (SPR). Preformed CsgB fibers were immobilized on a sensor chip. Soluble CsgA was able to interact with CsgB fibers shown by the increase of resonance units when CsgA was injected over the sensor chip. No obvious decay of resonance units was observed after injection, suggesting that the interaction between CsgA and CsgB fibers was non-reversible (Fig. 1F). These results suggest that WT CsgB rapidly polymerizes into an amyloid fiber that templates CsgA polymerization *in vitro*.

The ability of CsgB to template CsgA under physiologically relevant conditions was tested by adding purified, soluble CsgB to *csgA* and *csgB* mutant cells grown on YESCA plates. We have used this 'overlay assay' to measure the ability of cell surface localized CsgB to stimulate the polymerization of purified and exogenously added CsgA [30; 31]. In this case, purified soluble CsgB was spotted on to bacterial lawns of *csgA* or *csgB* cells grown under curli-inducing conditions, followed by an overnight incubation. The cells were then stained with Congo red to visualize amyloid formation [30; 31]. In comparison to the *csgA* mutant cells, the *csgB* mutants incubated with CsgB had a pronounced Congo red staining phenotype where the purified CsgB had been added (Fig. 2A). Thus, purified CsgB complemented the *csgB* mutant for Congo red binding when added to the cells exogenously. Using electron microscopy, we confirmed that fibers had formed when purified CsgB was incubated with the *csgB* mutants (Fig. 2B). To determine if the CsgA secreted from the CsgB-treated *csgB* mutants had formed detergent insoluble fibers, these cells were harvested and resuspended in the presence or absence of formic acid. The majority of CsgA in these samples required formic acid pretreatment to resolve the monomer, indicating that the protein was assembled into an SDS-insoluble and polymerized fiber form (Fig. 2C). Taken together, these results demonstrate that CsgB adopts an amyloid conformation more rapidly than the major subunit CsgA and this conformation is able to template CsgA polymerization near the cell surface.

In vivo contribution of the repeating units to CsgB function

CsgB contains a glutamine-asparagine rich domain that can be divided into five repeat sequences called r1, r2, r3, r4 and r5 (Fig. 3A) [27; 28]. Each repeating unit is predicted to contain two β-strands. The amino acid sequence of each repeating unit of CsgA and CsgB contain a high degree of similarity (Fig. 3A). In order to determine the contribution of each repeating unit to CsgB function *in vivo*, we constructed in-frame deletions of each repeating unit. When a *csgB* mutant strain expressing *csgB* constructs with deletions of r1, r2 or r3 ($CsgB^{\Delta r1}$, $CsgB^{\Delta r2}$, $CsgB^{\Delta r3}$) were grown under curli-inducing conditions on Congo red-containing agar plates, these mutants bound similar levels of Congo red as both WT cells and a *csgB* mutant complemented with WT *csgB* (Fig. 3B). Both $CsgB^{\Delta r1}$ and $CsgB^{\Delta r3}$ could be detected by western blot and increased amounts of $CsgB^{\Delta r1}$ and $CsgB^{\Delta r3}$ monomers were seen when the whole-cell samples were pretreated with FA (Fig. 3C top panel, lanes 6 and 10). The $CsgB^{\Delta r2}$ protein was not detected by western blot, because the CsgB antibody used here was raised using a peptide fragment found within r2 [36]. However, like the WT CsgB, $CsgB^{\Delta r1}$ and $CsgB^{\Delta r3}$ constructs, CsgA monomers could only be detected in whole-cell samples when the $CsgB^{\Delta r2}$ samples were pretreated with FA (Fig. 3.2C bottom panel, lanes 4, 6, 8, and 10). These results suggest the $CsgB^{\Delta r1}$, $CsgB^{\Delta r2}$, and $CsgB^{\Delta r3}$ constructs were able to convert soluble CsgA into a cell-associated SDS insoluble fiber. To confirm the presence of fibers, we prepared *csgB* mutants harboring each repeating unit deletion mutant for TEM. Consistent with the Congo red and western blot data, fibers were seen when *csgB* mutants harboring the $CsgB^{\Delta r1}$, $CsgB^{\Delta r2}$ and $CsgB^{\Delta r3}$ constructs were viewed by TEM, and these fibers were morphologically similar to WT curli fibers (Fig. 3D). Therefore, the r1, r2, and r3 deletion mutants were able to effectively complement the *csgB* mutant to produce cell-associated amyloid fibers.

Unlike the r1, r2 and r3 deletions, both the $CsgB^{\Delta r4}$ and $CsgB^{\Delta r5}$ constructs were unable to complement a *csgB* mutant for Congo red binding (Fig. 3B). To test for the stability of $CsgB^{\Delta r4}$ and $CsgB^{\Delta r5}$, cell lysates were probed with anti-CsgB antibody and no cell-associated $CsgB^{\Delta r4}$ or $CsgB^{\Delta r5}$ protein could be detected (Fig. 3C top panel, lanes 11–14). However, when whole cells and the underlying agar were collected, bands corresponding to the $CsgB^{\Delta r4}$ and $CsgB^{\Delta r5}$ constructs were observed (Fig. 3C middle panel, lanes 11–14). This indicated that both $CsgB^{\Delta r4}$ and $CsgB^{\Delta r5}$ were not cell associated, but were instead

secreted into the underlying agar. The soluble nature of these mutant proteins also renders them more sensitive to formic acid, which is manifested by an apparent decrease in protein stability (Fig. 3C middle panel, lanes 12 and 14). These results are also consistent with our previous report characterizing $CsgB^{\Delta r5}$ (previously referred to as $CsgB_{trunc}$) [34]. Soluble CsgA was detected when the underlying agar was collected along with the *csgB* cells harboring $CsgB^{\Delta r4}$ or $CsgB^{\Delta r5}$ (data not shown). Thus the $CsgB^{\Delta r4}$ and $CsgB^{\Delta r5}$ constructs do not alter CsgA stability. No fibers could be detected by TEM in samples of *csgB* cells expressing either $csgB^{\Delta r4}$ or $csgB^{\Delta r5}$ (Fig. 3D) [34]. These results suggest that the C-terminal portion of CsgB required for nucleator function *in vivo* includes both CsgB r4 and r5. The observation that both $csgB^{\Delta r4}$ and $csgB^{\Delta r5}$ are secreted away from the cell suggests that the last two CsgB repeating units are required to facilitate anchoring of the nucleator to the outer membrane.

The repeating unit deletion mutants polymerize in vitro

A possible explanation for the *in vivo* defect of the $CsgB^{\Delta r4}$ construct was that the 4th repeating unit is required for interaction with CsgA. To determine if $CsgB^{\Delta r4}$ could act as a template for CsgA polymerization and to characterize the *in vitro* characteristics of the other repeating unit mutants, we constructed expression plasmids for cytoplasmic purification of each of the CsgB repeating unit deletion mutants. Each repeating unit deletion, with the exception of $CsgB^{\Delta r4}$, formed SDS-insoluble cytoplasmic aggregates after induction (Fig. 4A). Soluble $CsgB^{\Delta r2}$, $CsgB^{\Delta r3}$, $CsgB^{\Delta r4}$ and $CsgB^{\Delta r5}$ were purified after treatment with 8 M GndHCl (data not shown). We were unable to purify $CsgB^{\Delta r1}$ (see materials and methods).

We monitored the *in vitro* polymerization of $CsgB^{\Delta r2}$, $CsgB^{\Delta r3}$, $CsgB^{\Delta r4}$ and $CsgB^{\Delta r5}$ using the ThT time course assay. The polymerization curve of $CsgB^{\Delta r5}$ displayed a two-hour lag phase, consistent with previously published results (Fig. 4B) [34]. The lag phase for $CsgB^{\Delta r5}$ was noticeably longer than that of WT, $CsgB^{\Delta r2}$, $CsgB^{\Delta r3}$, and $CsgB^{\Delta r4}$, which all exhibited no apparent lag phase on this time scale. This suggests that repeating unit r5 is required for rapid, WT-like polymerization of CsgB *in vitro*.

The normalized $CsgB^{\Delta r2}$ ThT polymerization profile demonstrated that $CsgB^{\Delta r2}$ polymerized as quickly as WT CsgB (Fig. 4B). However, the relative fluorescent units (RFUs) recorded for $CsgB^{\Delta r2}$ after twelve hours of polymerization were consistently lower than WT CsgB at the same time point (Fig. 4B inset), suggesting that $CsgB^{\Delta r2}$ might adopt an altered conformation. No gross morphological differences between $CsgB^{\Delta r2}$ fibers and WT CsgB fibers were observed when the fibers were viewed utilizing TEM (Fig. 1C and Fig. 4C top panel). We next tested the ability of the $CsgB^{\Delta r2}$ fibers to seed CsgA polymerization. Using a 14 μM concentration of CsgA, we observed a lag phase of five hours for CsgA by itself, which is consistent with previous reports that the CsgA lag phase is concentration-dependent [8]. At this concentration, only 3.5% (w/w) seed of WT CsgB was needed to eliminate the lag phase (Fig. 4D). A short lag phase of roughly 30 minutes was seen when 3.5% (w/w) $CsgB^{\Delta r2}$ fiber was added to the reaction mix, but no apparent lag phase was observed when the amount of seed was increased to 9% (w/w) $CsgB^{\Delta r2}$ pre-formed fiber (Fig. 4D). These observations suggest $CsgB^{\Delta r2}$ may be less efficient than WT CsgB at converting CsgA into SDS-insoluble fibers, however they are consistent with the *in vivo* results demonstrating SDS-insoluble CsgA fibers are formed in the presence of $CsgB^{\Delta r2}$ (Fig. 3).

Despite the inability to produce curli *in vivo*, the $CsgB^{\Delta r4}$ had a ThT fluorescence profile similar to WT CsgB *in vitro* (Fig. 4B). Fractions containing purified $CsgB^{\Delta r4}$ were incubated overnight and viewed by TEM to assess aggregate morphology. By this analysis, $CsgB^{\Delta r4}$ fibers appeared similar to WT CsgB fibers (Fig. 4C bottom panel). To determine if

the *in vivo* defect of CsgB$^{\Delta r4}$ could be attributed to an inability of CsgB$^{\Delta r4}$ to seed CsgA polymerization *in vitro*, pre-formed CsgB$^{\Delta r4}$ fibers were added to a CsgA polymerization reaction. A short lag phase of 30 minutes was observed when 3.5% (w/w) CsgB$^{\Delta r4}$ fibers were added to CsgA and no apparent lag phase could be detected when the amount of preformed fiber was increased to 8% (w/w) (Fig. 4D). These results demonstrate that CsgB$^{\Delta r4}$ formed amyloid fibers *in vitro* and that these CsgB$^{\Delta r4}$ fibers template *in vitro* CsgA polymerization. Thus the inability of CsgB$^{\Delta r4}$ to complement a *csgB* mutant cannot be fully explained by a defect of CsgB$^{\Delta r4}$ to template CsgA polymerization *in vitro*. These results suggest that like CsgA, CsgB may have more than one domain that acts to template CsgA polymerization *in vivo*. Alternatively, CsgB r4 may play a role in anchoring CsgB to the cell surface as CsgB$^{\Delta r4}$ was detected in the underlying agar *in vivo* (Fig. 2).

In order to gain a better understanding of the repeating unit(s) that have the potential to act as a template for CsgA polymerization we determined the ability of the individual CsgB repeating units to self-assemble using synthetic peptides composed of the amino acids found within each repeating unit. A similar approach was used to determine the repeating units of CsgA that facilitated CsgA polymerization. Synthetic peptides composed of the repeating units CsgA r1 and r5 were able to polymerize *in vitro*. CsgA r5 peptide polymerized with at a remarkable rate. Deleting CsgA r1 or CsgA r5 abrogated curli biogenesis *in vivo* highlighting the importance of these repeating units to CsgA polymerization [30]. The template-mediated polymerization hypothesis predicts that domains of CsgB that self-assemble will contribute to nucleator function. Therefore, we hypothesized that repeating units CsgB r5 and CsgB r4 would self assemble given their importance to *in vivo* curli biogenesis.

Synthetic peptides composed of amino acids found in each CsgB repeating unit were incubated with ThT to assess the self-assembly capability of each CsgB repeating unit. Peptides composed of the corresponding amino acid sequence of CsgB r1, CsgB r2 and CsgB r4 increased ThT fluorescence after a 24-hour incubation at room temperature, while peptides composed of the corresponding amino acid sequence of CsgB r3 and CsgB r5 did not result in ThT fluorescence over a 24 hour time period (Fig. 4E). Interestingly, deleting a repeating unit incapable of self-assembly into amyloid, CsgB r5, resulted in significant delay in CsgB polymerization *in vitro* (Fig. 4B). These results suggest that the initiation of CsgB polymerization via CsgB r5 does not require an amyloid-like self-assembly of this repeating unit. Taken together with the *in vivo* data demonstrating that CsgB$^{\Delta r5}$ is defective for nucleation, these findings imply that CsgB r5 might aid in the nucleating properties of CsgB by promoting CsgB polymerization in addition to its role of ensuring that CsgB is properly localized.

Discussion

Shewmaker *et al.* recently purified full-length CsgA and CsgB (i.e. versions of the proteins that would be expressed in the cytoplasm before processing by the Sec machinery) and demonstrated that both proteins self-assembled into fibers that contain the biochemical features of amyloid fibers [33]. Solid state NMR revealed that both CsgA and CsgB fibers are composed of parallel β–sheets that are not in-register. Together with the solid state NMR data, electron microscopy analysis suggests CsgA fibers and CsgB fibers consist of β–helix-like structure. This structure is different from the in-register parallel β–sheet structure shared among the yeast prions and human disease-associated amyloids. In their studies with CsgA and CsgB, Shewmaker *et al.* suggest that a functional amyloid may adopt a similar final amyloid structure [33]. Despite the conserved β-helix structure and high degree of similarity at the amino acid level our results demonstrate that CsgB has several unique features that distinguish it from CsgA. We demonstrate that these unique features facilitate the initial step

of curli fiber biogenesis, a process that occurs at the cell surface and shortens the lag phase of CsgA polymerization, thus increasing the efficiency of curli assembly at the correct cellular location.

WT CsgB polymerizes rapidly in vitro

At equal concentrations the lag phase of WT CsgB is shorter (20–30 minutes) than the two-hour lag phases that are observed when polymerization of both CsgA and CsgB$^{\Delta r5}$ is monitored (Fig. 1B and Fig. 3B). Our model predicts that CsgB is secreted to the cell surface where it rapidly adopts an amyloid fold that templates CsgA polymerization. CsgB amyloid fibers seeded CsgA polymerization *in vitro* (Fig. 1E) and freshly purified, soluble CsgB applied to *csgB* mutant cells was able to nucleate the CsgA secreted from these *csgB* mutant cells (Fig. 2). These data support the hypothesis that CsgB rapidly adopts an amyloid fold that templates CsgA polymerization at the cell surface.

Proteins associated with amyloid diseases aggregate relatively slowly *in vitro*, and the longer lag phases associated with the polymerization of these proteins have led to the hypothesis that cytotoxic amyloid precursors accumulate *in vivo* [37; 38; 39; 40; 41; 42; 43; 44; 45]. These precursors have been shown to compromise membrane integrity, leading to cell death [46; 47; 48; 49]. Functional amyloid biogenesis pathways proceed without compromising cell physiology. One strategy cells employ to reduce the accumulation of cytotoxic precursors is to promote the rapid conversion of innocuous monomers to stable amyloid fibrils. An example of this is the mammalian functional amyloid protein Pmel that polymerizes without a lag phase *in vitro* [11]. Our previous studies have demonstrated that CsgA polymerization *in vitro* has a consistent two-hour lag phase that is concentration dependent [8]. A potentially toxic intermediate is formed during the lag phase, but the addition of preformed CsgA fibers to freshly purified CsgA can eliminate the lag phase and the formation of this folding intermediate [8]. Therefore, we speculate that CsgB-mediated nucleation of CsgA promotes the conversion of CsgA from a soluble monomer to an ordered amyloid aggregate without allowing CsgA to sample the toxic oligomeric state that many amyloids are known to populate [8; 48; 50; 51]. Consistent with this, a mutant variant of CsgA that polymerizes independently of CsgB *in vivo* has potent cytotoxic activity [52].

The C-terminal repeating units of CsgB are essential for nucleator function

CsgA r1 and CsgA r5 deletion mutants are defective for polymerization *in vivo* and peptides composed of CsgA r1 and r5 self assemble *in vitro* [31]. CsgA r1 and r5 peptides also seed *in vitro* CsgA polymerization [31]. These findings supported our model that proposes that CsgA polymerization is mediated by the interaction of the terminal amyloidogenic repeating units CsgA r1 and CsgA r5.

In-frame deletions of CsgB repeating unit r4 and r5 are the most defective CsgB mutants (Fig. 3) suggesting the C-terminal portion of CsgB directs curli nucleation. We previously reported that the CsgB$^{\Delta r5}$ mutant was defective for nucleator activity *in vivo* due to mislocalization of the protein [34]. Synthetic peptides composed of CsgB r5 did not self assemble *in vitro* (Fig. 4E). The CsgB$^{\Delta r5}$ mutant also had the longest polymerization lag phase when compared to WT CsgB and the other CsgB repeating unit deletion mutants. These results suggest CsgB r5, which does not self-assemble, directs CsgB polymerization *in vitro*.

CsgA polymerization is inhibited when repeating units that can self-assemble are deleted [31]. However, deleting self-assembling CsgB repeating units, CsgB r2 and CsgB r4, did not affect CsgB polymerization *in vitro* (Fig. 4). The CsgB$^{\Delta r2}$ and CsgB$^{\Delta r4}$ mutants also seeded CsgA polymerization *in vitro* (Fig. 4). Deleting CsgB r4 abolished nucleator activity *in vivo*

despite having no effect on *in vitro* CsgB polymerization (Fig. 3). The CsgB$^{\Delta r4}$ mutant, like CsgB$^{\Delta r5}$, was secreted away from the cell (Fig. 3). Synthetic peptides composed of CsgB r 4 self-assembled *in vitro* (Fig. 4E). Taken together, these results underscore another difference between CsgA and CsgB. CsgA polymerization is directed by amyloidogenic repeating units located on either side of the predicted amyloid core domain (CsgA r1 and r5). CsgB nucleator function is directed by two repeating units located at the C-terminal portion of the amyloid core. Only one of these repeating units self-assembles *in vitro* (CsgB r4). Interestingly, the repeating unit that directs CsgB polymerization *in vitro*, CsgB r5, does not self-assemble into amyloid (Fig. 4). This property of CsgB r5 is not surprising given the importance of membrane localization to the function of CsgB, and the sensitivity membranes have to the toxic effect of amyloids in general. An amyloid-independent mechanism to facilitating the initiation of an amyloid fold would ensures membrane integrity is not compromised during polymerization. Future experiments will define the mechanism by which CsgB r5 facilitates the folding of CsgB.

CsgB self-assembles in vivo

In a *csgA* mutant CsgB remains SDS-soluble at the cell surface where it can initiate the polymerization of CsgA secreted from cells grown in close proximity[26; 53]. Bian and Normark demonstrated that CsgB fibers can be formed at the cell surface when CsgB is overexpressed [25]. These results suggest that CsgB expression is under transcriptional control that keeps the protein from self-assembling *in vivo*. We have shown that purified CsgB rapidly self-assembles *in vitro* (Fig. 1). When purified CsgB was added to *csgA* mutants, there was a modest increase of Congo red binding in the area where CsgB had been applied (Fig. 2A). However, within this area fibers were not observed by EM and CsgB remained SDS-soluble (data not shown). These results suggest that interactions with the membrane or a membrane-localized protein may keep CsgB from polymerizing *in vivo*. The chaperone-like protein CsgF ensures the proper localization of curli biogenesis [53]. CsgF is the most likely candidate for interacting with CsgB, but a direct CsgB-CsgF interaction has not been demonstrated experimentally. Determining the molecular details of the CsgB-membrane interaction will increase our understanding of how *E. coli* keeps CsgB from polymerizing on the cell surface.

Curli are among a class of microbial functional amyloids that promote the formation of multicellular communities[13; 54; 55; 56; 57]. During amyloid formation, soluble peptides can assemble into structurally conserved oligomers before adopting the final amyloid fiber conformation [48]. Lipid membranes are particularly sensitive to the oligomeric intermediates formed during amyloid polymerization [58]. We speculate that dedicated amyloid nucleator proteins like CsgB stimulate the transition of CsgA from the soluble monomeric state to the final amyloid fiber, thus minimizing the chance for membrane-toxic oligomers to form that might compromise the integrity of the outer membrane. To date, a dedicated amyloidogenic nucleator of the extracellular Gram positive and yeast functional amyloids has not been identified [56; 59]. Future experiments will define the nucleation events that initiate the polymerization of this class of functional amyloids, but it is tempting to speculate that a dedicated amyloidogenic nucleator is essential for Gram negative bacteria to assemble a nontoxic, cell-associated amyloid fiber. The molecular basis of the CsgB-membrane interaction will lead to novel insights into how Gram negative bacteria avoid the accumulation of cytotoxic intermediates produced during amyloid fiber biogenesis.

The molecular events that initiate amyloid biogenesis *in vivo* are not entirely understood. Curli biogenesis represents an elegant functional amyloid biosynthetic pathway that faithfully assembles an amyloid on the cell surface without causing appreciable cytotoxicity. Our results support the template-mediated polymerization model of curli biogenesis, where CsgB rapidly adopts an amyloid-like fold that initiates the folding of soluble CsgA as it

comes in contact with the cell surface. This process is directed by the C-terminal repeating units of CsgB. Further study of the nucleation event in curli biogenesis, from both *in vivo* and *in vitro* perspectives, may provide alternative approaches for inhibiting disease associated amyloid biogenesis.

Materials and methods

Bacterial Growth

For protein expression and general strain propagation bacteria were cultured in LB broth. To induce curli production, bacteria were grown for 48 hours at 26° C on yeast extract casamino acids (YESCA) plates [10]. Curli production was monitored by using Congo red-containing YESCA plates [10]. When necessary growth media was supplemented with antibiotics at the following concentrations: kanamycin 50 μg/ml or ampillicin, 100 μg/ml.

Bacterial Strains and Plasmids

MC4100 was the WT strain used [60]. The other strains and plasmids used in this study can be found in table S1. Primers used to construct the plasmids in this study can be found in table S2. The repeating unit deletions and point mutants were constructed using synthesis by overlapping ends PCR. PCR was performed using standard techniques and the primers listed in table S3. To test the ability of the *csgB* mutants to complement the *csgB* mutant strain the mutated sequences were all subcloned into pLR2, a plasmid that contains the native *csgBA* promoter, using *NcoI* and *BamHI* restriction sites found at the 5′ and 3′ end respectively [36]. To express and purify cytoplasmic (i.e., lacking the N-terminal *sec*-signal sequence) WT CsgB and the repeating unit deletions, PCR-amplified sequences including 6 histidine residues at the C-terminus were subcloned into pET11d (Novagen, Darmstadt, Germany) using NcoI and BamHI restriction sites. Our attempts to purify proteins using a denaturing protocol described below were hindered by a contaminating protein of approximately 30 kDa. We identified this protein as SlyD, a protein enriched with histidine residues at the C-terminus, by mass spectrophotometry analysis (Michigan Proteome Consortium). In order to eliminate this contamination we P1 transduced the *slyD::aph* allele from the Keio collection strain, JW3311, into our expression strain NEB 3016 [61; 62]. We named the resulting strain NDH 471

CsgA and CsgB Protein purification

NDH 471 (NEB 3016 *slyD::aph*) cells harboring a pET11d vector containing polyhistidine-tagged cytoplasmic versions of CsgA, CsgB, or the CsgB repeating unit deletions mutants were grown at 37° C to 0.9 OD_{600}. The cells were induced with 0.5 mM isopropyl-β-D-thiogalactoside (IPTG) and induction proceeded at 37° C for an hour. Cells were collected by centrifugation and the pellets were stored at −80° C. The cells were chemically lysed using 8 M GndHCl buffered with 50 mM potassium phosphate buffer (KPi) pH7.2. A total of 75 ml of lysis solution was used per pellet generated from a 500 ml culture. The lysate was incubated at room temperature with magnetic stirring for 24 hours. The insoluble portion of the lysate was removed by centrifuging at 10,500 × g for 15 minutes and the resulting supernatant was sonicated 5 times, each time for 15 seconds. Sonication was applied at 5 amplitudes. The samples were incubated for 2 minutes on ice in between bursts. The supernatant was then centrifuged again at 10,500 × g for 15 min. HIS-Select ™ HF NiNTA (Sigma Aldrich, Atlanta, GA) was added to the supernatant and this mixture was incubated for 1 hour at room temperature with rocking. The polyhistidine-tagged proteins were affinity purified by collecting the nickel beads as the mixture passed through a Kontes column. The beads were washed with 50 mM KPi pH7.2 to eliminate the GndHCl and then washed with 50 mM KPi containing 12.5 mM imidazole pH7.2 to elute contaminating proteins that bound to the nickel beads. His-tagged proteins were eluted from the column

using 125 mM imidazole in 50 mM KPi pH 7.2. Fractions were collected and analyzed for the presence of protein by SDS-PAGE. Protein concentration was determined by the BCA assay (Thermo Scientific, Rockford, IL). We were not able to purify $CsgB^{\Delta r1}$. A significant amount of $CsgB^{\Delta r1}$ protein was found to be SDS insoluble even after the cells were resuspended in 8 M GndHCl (data not shown).

Thioflavin-T (ThT) Assay

Proteins were mixed with 20 μM ThT in 96-well plates in duplicate and incubated at room temperature. Every 10 minutes samples were excited at 438 nm and fluorescence emitted 495 nm with a 475 nm cutoff was measured using a Spectramax M2 plate reader (Molecular Devices, Sunnyvale, CA). Samples were shaken for 5 seconds before each read. Due to the differences in preparation–to-preparation protein yield, a representative ThT kinetic graph taken from a series of at least three ThT assays is shown. The net RFUs generated by a protein at a specific concentration after a 24 hour incubation from a given preparation were consistent from protein preparation to protein preparation. ThT fluorescence was normalized by averaging the duplicate samples and using $(F_i - F_o)/(F_{max} - F_o)$ were F_o was the ThT background intensity (fluorescence arbitrary unit), F_i was the ThT intensity of samples, and F_{max} was the maximum ThT intensity of the reaction. Samples used to seed CsgA were sonicated using a sonic dismembrator (Fisher Model 100; Fisher, Pittsburg, PA) for three 15-second bursts on ice.

BIAcore Binding Assay

A BIAcore3000 (GE Appliance) was used to analyze the seeding reaction. Mature CsgB or CsgA fibers were sonicated (Sonicator XL2020, Misonix) on ice with 4 times of 15 second burst at power two and 50 second pause and diluted with 10 mM sodium acetate buffer, pH5 by 10 fold. Sonicated fibers were then immobilized on a CM5 chip (GE Appliance) pre-activated with 1:1 (v/v) mixture of 0.4 M of 1-ethyl-3-(3-dimethylpropyl)-carboiimide (EDC) and 0.1 M N-hydroxysuccinimide (NHS) to reach the immobilization of 3000 resonance units. A blank flow cell was prepared in absence of seeds. This flow cell was used as the negative control. Excessive reactive groups were deactivated with 1M ethanolamine-HCl, pH 8.5. To test interactions between monomeric CsgA and the CsgA or CsgB seeds, 40 μl 0.25 μM monomeric CsgA was injected over the sensor chip at a flow rate of 50 μl/minute and the response was recorded in resonance units.

Overlay assay

Cells were grown under curli inducing conditions as previously described for 24 hours on YESCA plates. Purified CsgB (10 ul) was pipetted onto the bacterial lawn and incubated at 26° C for an additional 24 hours. Congo red dye (10 mg/ml) was then applied to the bacterial lawn-CsgB mixture for 10 minutes. The dye was decanted and the bacterial lawns were carefully washed twice with 50 mM KPi buffer pH 7.2.

Transmission Electron Microscopy (TEM)

Samples (10 μL) were placed on glow discharged, Formvar-coated copper grids (Ernest F. Fullman, Inc., Latham, NY) for 2 minutes, washed twice briefly (10 seconds) with deionized water, and negatively stained with 2% uranyl acetate for 90 seconds. Samples were viewed using a Phillips CM-100 transmission electron microscope at 60kv.

SDS/PAGE and Western Blotting

Bacteria whole cell lysates and agar plugs were prepared and probed for both CsgA and CsgB by using previously described methods [34; 36].

Peptide preparation

Peptides were chemically synthesized (Proteintech Group, Chicago, IL). Purity was greater than 90% as measured by high pressure liquid chromatography, and size was confirmed by mass spectroscopy (Proteintech Group, Chicago, IL). Lyophilized peptide (1 mg) was dissolved in 8 M GndHCl (1ml) buffered by 50 mM KPi pH 7.2. The suspension was incubated at room temperature for 1 hour with rocking. In order to remove the 8 M GndHCl and collect the soluble peptide, the sample was passed through a Sephadex G10 (GE Healthcare, Brentwood, TN) column that was balanced in 50 mM KPi pH 7.2. The BCA assay was used to assess peptide concentration and polymerization was monitored by ThT.

Supplementary Material

Refer to Web version on PubMed Central for supplementary material.

Acknowledgments

We would like to thank members of the Chapman and Scott Hultgren laboratories for helpful discussions and review of this manuscript. We also thank the Almqvist lab and Emma Andersson for technical help with the BIAcore. This work was supported by NIH AI 073847 and by the Umeå University Linnaeus Foundation.

Abbreviations

FA	formic acid
WT	wild type
Gnd HCl	Guandine Hydrochloride
TEM	Transmission electron microscopy

References

1. Cohen FE, Kelly JW. Therapeutic approaches to protein-misfolding diseases. Nature. 2003; 426:905–9. [PubMed: 14685252]
2. Chiti F, Dobson CM. Protein misfolding, functional amyloid, and human disease. Annu Rev Biochem. 2006; 75:333–66. [PubMed: 16756495]
3. Jarrett JT, Lansbury PT Jr. Seeding “one-dimensional crystallization” of amyloid: a pathogenic mechanism in Alzheimer’s disease and scrapie? Cell. 1993; 73:1055–8. [PubMed: 8513491]
4. Lomakin A, Chung DS, Benedek GB, Kirschner DA, Teplow DB. On the nucleation and growth of amyloid beta-protein fibrils: detection of nuclei and quantitation of rate constants. Proc Natl Acad Sci U S A. 1996; 93:1125–9. [PubMed: 8577726]
5. Pedersen JS, Christensen G, Otzen DE. Modulation of S6 fibrillation by unfolding rates and gatekeeper residues. J Mol Biol. 2004; 341:575–88. [PubMed: 15276845]
6. Serio TR, Cashikar AG, Kowal AS, Sawicki GJ, Moslehi JJ, Serpell L, Arnsdorf MF, Lindquist SL. Nucleated conformational conversion and the replication of conformational information by a prion determinant. Science. 2000; 289:1317–21. [PubMed: 10958771]
7. Uversky VN, Li J, Souillac P, Millett IS, Doniach S, Jakes R, Goedert M, Fink AL. Biophysical properties of the synucleins and their propensities to fibrillate: inhibition of alpha-synuclein assembly by beta- and gamma-synucleins. J Biol Chem. 2002; 277:11970–8. [PubMed: 11812782]
8. Wang X, Smith DR, Jones JW, Chapman MR. In Vitro Polymerization of a Functional Escherichia coli Amyloid Protein. J Biol Chem. 2007; 282:3713–9. [PubMed: 17164238]
9. Rochet JC, Lansbury PT Jr. Amyloid fibrillogenesis: themes and variations. Curr Opin Struct Biol. 2000; 10:60–8. [PubMed: 10679462]

10. Chapman MR, Robinson LS, Pinkner JS, Roth R, Heuser J, Hammar M, Normark S, Hultgren SJ. Role of Escherichia coli curli operons in directing amyloid fiber formation. Science. 2002; 295:851–5. [PubMed: 11823641]
11. Fowler DM, Koulov AV, Alory-Jost C, Marks MS, Balch WE, Kelly JW. Functional amyloid formation within mammalian tissue. PLoS Biol. 2006; 4:e6. [PubMed: 16300414]
12. Serio TR, Lindquist SL. The yeast prion [PSI+]: molecular insights and functional consequences. Adv Protein Chem. 2001; 59:391–412. [PubMed: 11868278]
13. Wang X, Rochon M, Lamprokostopoulou A, Lunsdorf H, Nimtz M, Romling U. Impact of biofilm matrix components on interaction of commensal Escherichia coli with the gastrointestinal cell line HT-29. Cell Mol Life Sci. 2006; 63:2352–63. [PubMed: 16952050]
14. Barnhart MM, Chapman MR. Curli biogenesis and function. Annu Rev Microbiol. 2006; 60:131–47. [PubMed: 16704339]
15. Gerstel U, Romling U. The csgD promoter, a control unit for biofilm formation in Salmonella typhimurium. Res Microbiol. 2003; 154:659–67. [PubMed: 14643403]
16. Olsen A, Jonsson A, Normark S. Fibronectin binding mediated by a novel class of surface organelles on Escherichia coli. Nature. 1989; 338:652–5. [PubMed: 2649795]
17. Uhlich GA, Cooke PH, Solomon EB. Analyses of the red-dry-rough phenotype of an Escherichia coli O157:H7 strain and its role in biofilm formation and resistance to antibacterial agents. Appl Environ Microbiol. 2006; 72:2564–72. [PubMed: 16597958]
18. Vidal O, Longin R, Prigent-Combaret C, Dorel C, Hooreman M, Lejeune P. Isolation of an Escherichia coli K-12 mutant strain able to form biofilms on inert surfaces: involvement of a new ompR allele that increases curli expression. J Bacteriol. 1998; 180:2442–9. [PubMed: 9573197]
19. Cegelski L, Marshall GR, Eldridge GR, Hultgren SJ. The biology and future prospects of antivirulence therapies. Nat Rev Microbiol. 2008; 6:17–27. [PubMed: 18079741]
20. Clatworthy AE, Pierson E, Hung DT. Targeting virulence: a new paradigm for antimicrobial therapy. Nat Chem Biol. 2007; 3:541–8. [PubMed: 17710100]
21. Lee YM, Almqvist F, Hultgren SJ. Targeting virulence for antimicrobial chemotherapy. Curr Opin Pharmacol. 2003; 3:513–9. [PubMed: 14559097]
22. Cegelski L, Pinkner JS, Hammer ND, Cusumano CK, Hung CS, Chorell E, Aberg V, Walker JN, Seed PC, Almqvist F, Chapman MR, Hultgren SJ. Small-molecule inhibitors target Escherichia coli amyloid biogenesis and biofilm formation. Nat Chem Biol. 2009; 5:913–9. [PubMed: 19915538]
23. Chorell E, Bengtsson C, Banchelin TS, Das P, Uvell H, Sinha AK, Pinkner JS, Hultgren SJ, Almqvist F. Synthesis and application of a bromomethyl substituted scaffold to be used for efficient optimization of anti-virulence activity. Eur J Med Chem. 2011; 46:1103–1116. [PubMed: 21316127]
24. Horvath I, Weise CF, Andersson EK, Chorell E, Sellstedt M, Bengtsson C, Olofsson A, Hultgren SJ, Chapman M, Wolf-Watz M, Almqvist F, Wittung-Stafshede P. Mechanisms of Protein Oligomerization: Inhibitor of Functional Amyloids Templates alpha-Synuclein Fibrillation. J Am Chem Soc. 2012
25. Bian Z, Normark S. Nucleator function of CsgB for the assembly of adhesive surface organelles in Escherichia coli. Embo J. 1997; 16:5827–36. [PubMed: 9312041]
26. Hammar M, Bian Z, Normark S. Nucleator-dependent intercellular assembly of adhesive curli organelles in Escherichia coli. Proc Natl Acad Sci U S A. 1996; 93:6562–6. [PubMed: 8692856]
27. White AP, Collinson SK, Banser PA, Gibson DL, Paetzel M, Strynadka NC, Kay WW. Structure and characterization of AgfB from Salmonella enteritidis thin aggregative fimbriae. J Mol Biol. 2001; 311:735–49. [PubMed: 11518527]
28. Hammar M, Arnqvist A, Bian Z, Olsen A, Normark S. Expression of two csg operons is required for production of fibronectin- and congo red-binding curli polymers in Escherichia coli K-12. Mol Microbiol. 1995; 18:661–70. [PubMed: 8817489]
29. Loferer H, Hammar M, Normark S. Availability of the fibre subunit CsgA and the nucleator protein CsgB during assembly of fibronectin-binding curli is limited by the intracellular concentration of the novel lipoprotein CsgG. Mol Microbiol. 1997; 26:11–23. [PubMed: 9383186]

30. Wang X, Chapman MR. Sequence determinants of bacterial amyloid formation. J Mol Biol. 2008; 380:570–80. [PubMed: 18565345]

31. Wang X, Hammer ND, Chapman MR. The molecular basis of functional bacterial amyloid polymerization and nucleation. J Biol Chem. 2008; 283:21530–9. [PubMed: 18508760]

32. Collinson SK, Parker JM, Hodges RS, Kay WW. Structural predictions of AgfA, the insoluble fimbrial subunit of Salmonella thin aggregative fimbriae. J Mol Biol. 1999; 290:741–56. [PubMed: 10395827]

33. Shewmaker F, McGlinchey RP, Thurber KR, McPhie P, Dyda F, Tycko R, Wickner RB. The functional curli amyloid is not based on in-register parallel beta-sheet structure. J Biol Chem. 2009; 284:25065–76. [PubMed: 19574225]

34. Hammer ND, Schmidt JC, Chapman MR. The curli nucleator protein, CsgB, contains an amyloidogenic domain that directs CsgA polymerization. Proc Natl Acad Sci U S A. 2007; 104:12494–9. [PubMed: 17636121]

35. Nenninger AA, Robinson LS, Hammer ND, Epstein EA, Badtke MP, Hultgren SJ, Chapman MR. CsgE is a curli secretion specificity factor that prevents amyloid fibre aggregation. Mol Microbiol. 2011; 81:486–99. [PubMed: 21645131]

36. Robinson LS, Ashman EM, Hultgren SJ, Chapman MR. Secretion of curli fibre subunits is mediated by the outer membrane-localized CsgG protein. Mol Microbiol. 2006; 59:870–81. [PubMed: 16420357]

37. Bucciantini M, Giannoni E, Chiti F, Baroni F, Formigli L, Zurdo J, Taddei N, Ramponi G, Dobson CM, Stefani M. Inherent toxicity of aggregates implies a common mechanism for protein misfolding diseases. Nature. 2002; 416:507–11. [PubMed: 11932737]

38. Larson J, Lynch G, Games D, Seubert P. Alterations in synaptic transmission and long-term potentiation in hippocampal slices from young and aged PDAPP mice. Brain Res. 1999; 840:23–35. [PubMed: 10517949]

39. Lue LF, Kuo YM, Roher AE, Brachova L, Shen Y, Sue L, Beach T, Kurth JH, Rydel RE, Rogers J. Soluble amyloid beta peptide concentration as a predictor of synaptic change in Alzheimer's disease. Am J Pathol. 1999; 155:853–62. [PubMed: 10487842]

40. Malisauskas M, Ostman J, Darinskas A, Zamotin V, Liutkevicius E, Lundgren E, Morozova-Roche LA. Does the cytotoxic effect of transient amyloid oligomers from common equine lysozyme in vitro imply innate amyloid toxicity? J Biol Chem. 2005; 280:6269–75. [PubMed: 15576361]

41. McLean CA, Cherny RA, Fraser FW, Fuller SJ, Smith MJ, Beyreuther K, Bush AI, Masters CL. Soluble pool of Abeta amyloid as a determinant of severity of neurodegeneration in Alzheimer's disease. Ann Neurol. 1999; 46:860–6. [PubMed: 10589538]

42. Moechars D, Dewachter I, Lorent K, Reverse D, Baekelandt V, Naidu A, Tesseur I, Spittaels K, Haute CV, Checler F, Godaux E, Cordell B, Van Leuven F. Early phenotypic changes in transgenic mice that overexpress different mutants of amyloid precursor protein in brain. J Biol Chem. 1999; 274:6483–92. [PubMed: 10037741]

43. Sirangelo I, Malmo C, Iannuzzi C, Mezzogiorno A, Bianco MR, Papa M, Irace G. Fibrillogenesis and cytotoxic activity of the amyloid-forming apomyoglobin mutant W7FW14F. J Biol Chem. 2004; 279:13183–9. [PubMed: 14701846]

44. Sousa MM, Cardoso I, Fernandes R, Guimaraes A, Saraiva MJ. Deposition of transthyretin in early stages of familial amyloidotic polyneuropathy: evidence for toxicity of nonfibrillar aggregates. Am J Pathol. 2001; 159:1993–2000. [PubMed: 11733349]

45. Wang J, Dickson DW, Trojanowski JQ, Lee VM. The levels of soluble versus insoluble brain Abeta distinguish Alzheimer's disease from normal and pathologic aging. Exp Neurol. 1999; 158:328–37. [PubMed: 10415140]

46. Bokvist M, Lindstrom F, Watts A, Grobner G. Two types of Alzheimer's beta-amyloid (1–40) peptide membrane interactions: aggregation preventing transmembrane anchoring versus accelerated surface fibril formation. J Mol Biol. 2004; 335:1039–49. [PubMed: 14698298]

47. Cecchi C, Baglioni S, Fiorillo C, Pensalfini A, Liguri G, Nosi D, Rigacci S, Bucciantini M, Stefani M. Insights into the molecular basis of the differing susceptibility of varying cell types to the toxicity of amyloid aggregates. J Cell Sci. 2005; 118:3459–70. [PubMed: 16079288]

48. Kayed R, Head E, Thompson JL, McIntire TM, Milton SC, Cotman CW, Glabe CG. Common structure of soluble amyloid oligomers implies common mechanism of pathogenesis. Science. 2003; 300:486–9. [PubMed: 12702875]
49. Stefani M, Dobson CM. Protein aggregation and aggregate toxicity: new insights into protein folding, misfolding diseases and biological evolution. J Mol Med. 2003; 81:678–99. [PubMed: 12942175]
50. Bieschke J, Herbst M, Wiglenda T, Friedrich RP, Boeddrich A, Schiele F, Kleckers D, Lopez Del Amo JM, Gruning BA, Wang Q, Schmidt MR, Lurz R, Anwyl R, Schnoegl S, Fandrich M, Frank RF, Reif B, Gunther S, Walsh DM, Wanker EE. Small-molecule conversion of toxic oligomers to nontoxic beta-sheet-rich amyloid fibrils. Nat Chem Biol. 2011; 8:93–101. [PubMed: 22101602]
51. Shorter J, Lindquist S. Hsp104 catalyzes formation and elimination of self-replicating Sup35 prion conformers. Science. 2004; 304:1793–7. [PubMed: 15155912]
52. Wang X, Zhou Y, Ren JJ, Hammer ND, Chapman MR. Gatekeeper residues in the major curlin subunit modulate bacterial amyloid fiber biogenesis. Proc Natl Acad Sci U S A. 107:163–8. [PubMed: 19966296]
53. Nenninger AA, Robinson LS, Hultgren SJ. Localized and efficient curli nucleation requires the chaperone-like amyloid assembly protein CsgF. Proc Natl Acad Sci U S A. 2009; 106:900–5. [PubMed: 19131513]
54. Ramsook CB, Tan C, Garcia MC, Fung R, Soybelman G, Henry R, Litewka A, O'Meally S, Otoo HN, Khalaf RA, Dranginis AM, Gaur NK, Klotz SA, Rauceo JM, Jue CK, Lipke PN. Yeast cell adhesion molecules have functional amyloid-forming sequences. Eukaryot Cell. 2010; 9:393–404. [PubMed: 20038605]
55. Otoo HN, Lee KG, Qiu W, Lipke PN. Candida albicans Als adhesins have conserved amyloid-forming sequences. Eukaryot Cell. 2008; 7:776–82. [PubMed: 18083824]
56. Romero D, Vlamakis H, Losick R, Kolter R. An accessory protein required for anchoring and assembly of amyloid fibres in B. subtilis biofilms. Mol Microbiol. 2011; 80:1155–68. [PubMed: 21477127]
57. Romero D, Aguilar C, Losick R, Kolter R. Amyloid fibers provide structural integrity to Bacillus subtilis biofilms. Proc Natl Acad Sci U S A. 2010; 107:2230–4. [PubMed: 20080671]
58. Kayed R, Sokolov Y, Edmonds B, McIntire TM, Milton SC, Hall JE, Glabe CG. Permeabilization of lipid bilayers is a common conformation-dependent activity of soluble amyloid oligomers in protein misfolding diseases. J Biol Chem. 2004; 279:46363–6. [PubMed: 15385542]
59. de Jong W, Wosten HA, Dijkhuizen L, Claessen D. Attachment of Streptomyces coelicolor is mediated by amyloidal fimbriae that are anchored to the cell surface via cellulose. Mol Microbiol. 2009; 73:1128–40. [PubMed: 19682261]
60. Casadaban MJ. Transposition and fusion of the lac genes to selected promoters in Escherichia coli using bacteriophage lambda and Mu. J Mol Biol. 1976; 104:541–55. [PubMed: 781293]
61. Baba T, Ara T, Hasegawa M, Takai Y, Okumura Y, Baba M, Datsenko KA, Tomita M, Wanner BL, Mori H. Construction of Escherichia coli K-12 in-frame, single-gene knockout mutants: the Keio collection. Mol Syst Biol. 2006; 2:2006 0008.
62. Goldberg RB, Bender RA, Streicher SL. Direct selection for P1-sensitive mutants of enteric bacteria. J Bacteriol. 1974; 118:810–4. [PubMed: 4598005]

Highlights

- The polymerization of wild type CsgB has not been biochemically characterized.
- Wild type CsgB polymerizes with rapid kinetics.
- The fourth and fifth repeating units of CsgB are required for in vivo function.
- Synthetic peptide composed of the fifth repeating unit domain do not self assemble.
- The rapid self assembly of CsgB is dependent upon a non-aggregative domain.

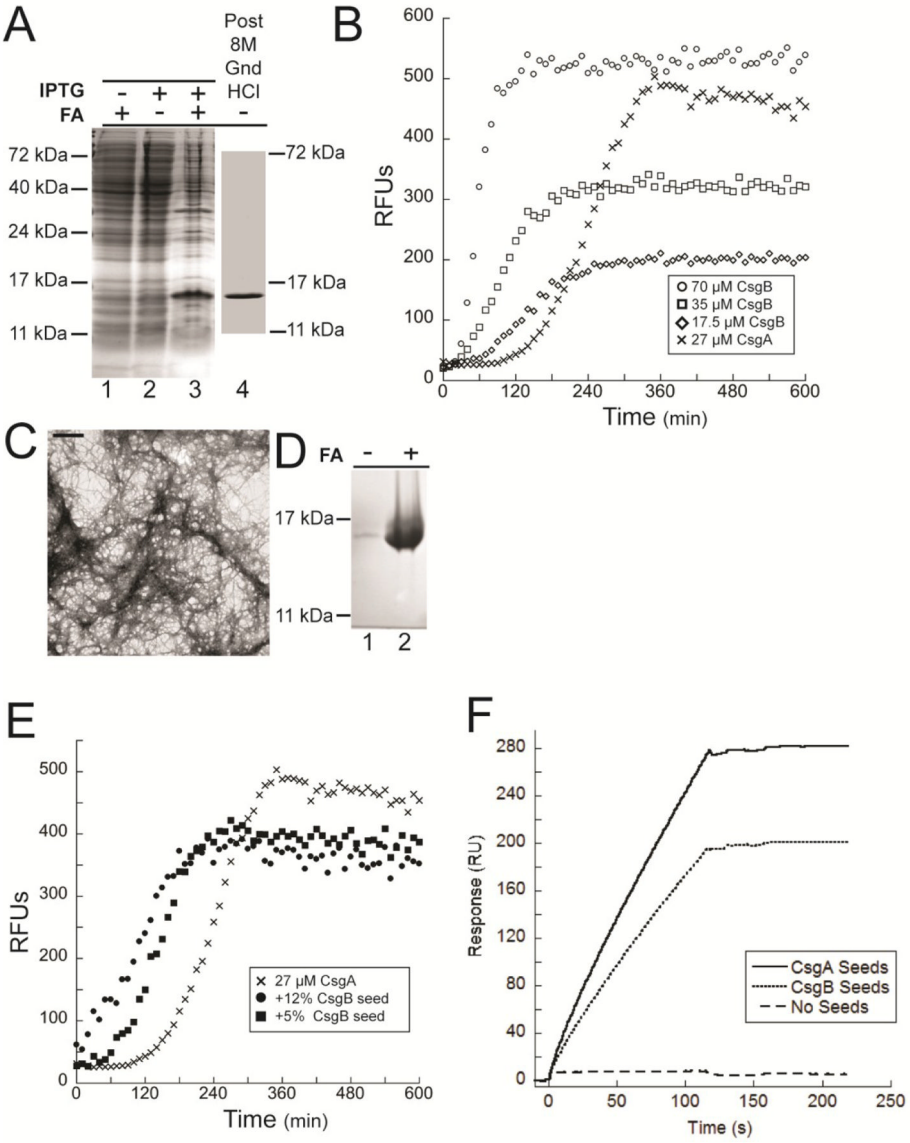

Figure 1. Biochemical and physiological properties of WT CsgB

(A) Coomassie stained SDS-PAGE of OD600 normalized cell lysates pre-induction (IPTG −) or post-induction (IPTG +) lanes 1 through 3. Cells were resuspended in SDS loading buffer (FA −) or pretreated with formic acid (FA+). CsgB was solubilized post purification by incubation in 8 M guanidine HCl (Lane 4). (B) Representative ThT kinetic plot of 70 μM (○), 35 μM (□), or 17.5 μM (◇) purified CsgB and 27 μM purified CsgA (X). Relative fluorescent units (RFUs) emitted at 495 nm were recorded every 10 min. after excitation at 438 nm. (C) TEM of 65 μM CsgB incubated at room temperature for 24 hours. The scale bar represents 500 nm. (D) Coomassie stained SDS-PAGE of 65 μM CsgB polymerized into fibers, centrifuged and resuspended in SDS loading buffer with (+) or without (−) prior formic acid (FA) treatment. (E) ThT kinetic plot of 27 μM CsgA (X), 27 μM CsgA and +5% w/w WT CsgB seeds (●) and 27μM CsgA + 12% w/w WT CsgB seeds (■). (F) Surface plasmon resonance (SPR) sensorgrams of interactions between monomeric CsgA and CsgA seeds or CsgB seeds. 0.25μM fresh monomeric CsgA was flow over the CM5

chip immobilized with 3uM CsgA seeds, 3.5μM CsgB seeds or no seeds. The interaction was recorded in resonance units.

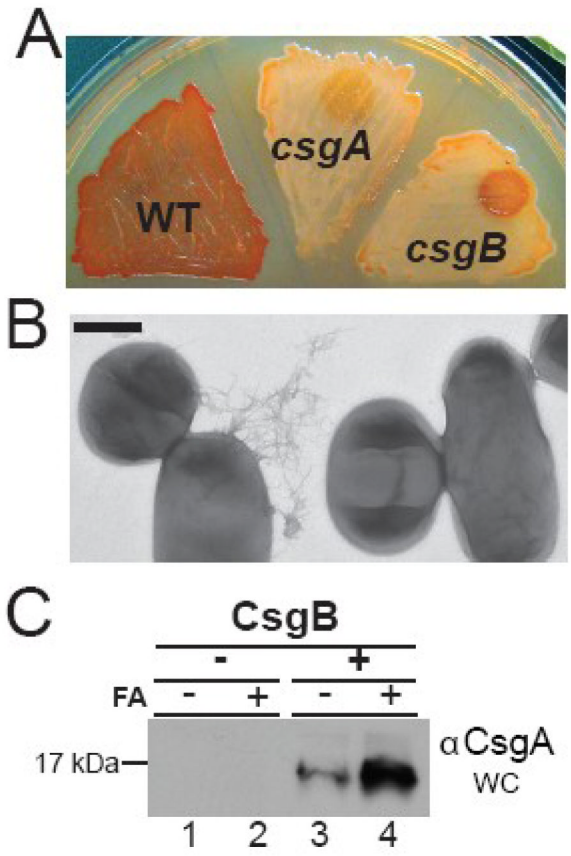

Figure 2. Exogenously added CsgB functions as a nucleator

(A) 10 ul of 37 μM purified CsgB was overlaid on *csgA* and *csgB* mutants that had been grown for 24 hours, and then stained with Congo red dye after an additional 24-hour incubation at 26°C. WT cells are shown as a positive staining control. (B) TEM of *csgB* cells that were incubated with 37 μM purified CsgB. The scale bar represents 500nm. (C) CsgA western blot analysis of a whole cell (WC) lysate of the *csgB* cells in (A) that were incubated in the absence of CsgB (Lanes 1 and 2) or presence of CsgB (lanes 3 and 4). Samples were resuspended in SDS loading buffer with (+) or without (−) formic acid (FA) pretreatment.

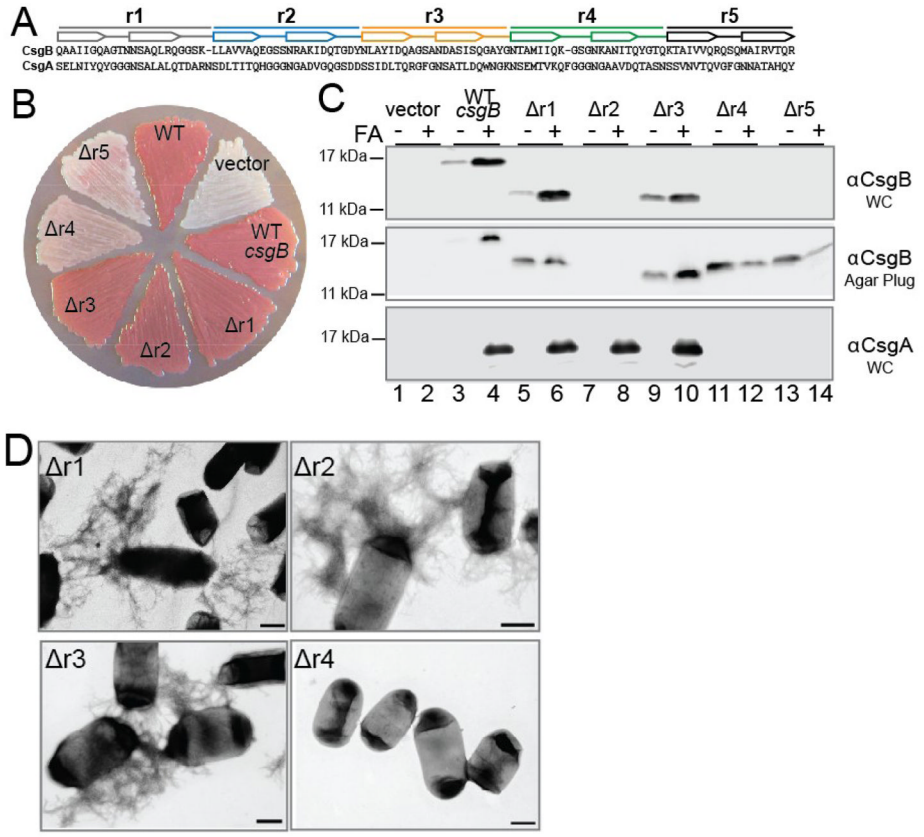

Figure 3. Contribution of each repeating unit to CsgB function *in vivo*

(A) Amino acid sequence alignment of the CsgA and CsgB repeating units. Each repeating unit contains two predicted β-sheets (arrows). (B) Congo red binding phenotype of MC4100 (WT), or *csgB* harboring a vector control plasmid (vector), a plasmid vector containing WT *csgB*, $csgB^{\Delta r1}$ (Δr1), $csgB^{\Delta r2}$ (Δr2), $csgB^{\Delta r3}$ (Δr3), $csgB^{\Delta r4}$ (Δr4) or $csgB^{\Delta r5}$ (Δr5). (C) Western blot analysis of a *csgB* mutant strain harboring vector control (vector lanes 1 and 2), a plasmid vector containing WT *csgB* (lanes 3 and 4), $csgB^{\Delta r1}$ (Δr1 lanes 5 and 6), $csgB^{\Delta r2}$ (Δr2 lanes 7 and 8), $csgB^{\Delta r3}$ (Δr3 lanes 9 and 10), $csgB^{\Delta r4}$ (Δr4 lanes 11 and 12) or $csgB^{\Delta r5}$ (Δr5 lanes 13 and 14). Samples were resuspended in SDS loading buffer with (+) or without (−) formic acid (FA) pretreatment. The top two panels are blots probed with anti-CsgB antibody. The bottom panel is a blot probed with anti-CsgA antibody. Whole cells (WC) samples are represented in the first and third panel, while samples containing whole cells and the underlying agar are represented in the second panel. (D) TEM of *csgB* mutants harboring $CsgB^{\Delta r1}$ (Δr1), $CsgB^{\Delta r2}$ (Δr2), $CsgB^{\Delta r3}$ (Δr3), or $CsgB^{\Delta r4}$ (Δr4) grown under curli-inducing conditions. The scale bars represent 500 nm.

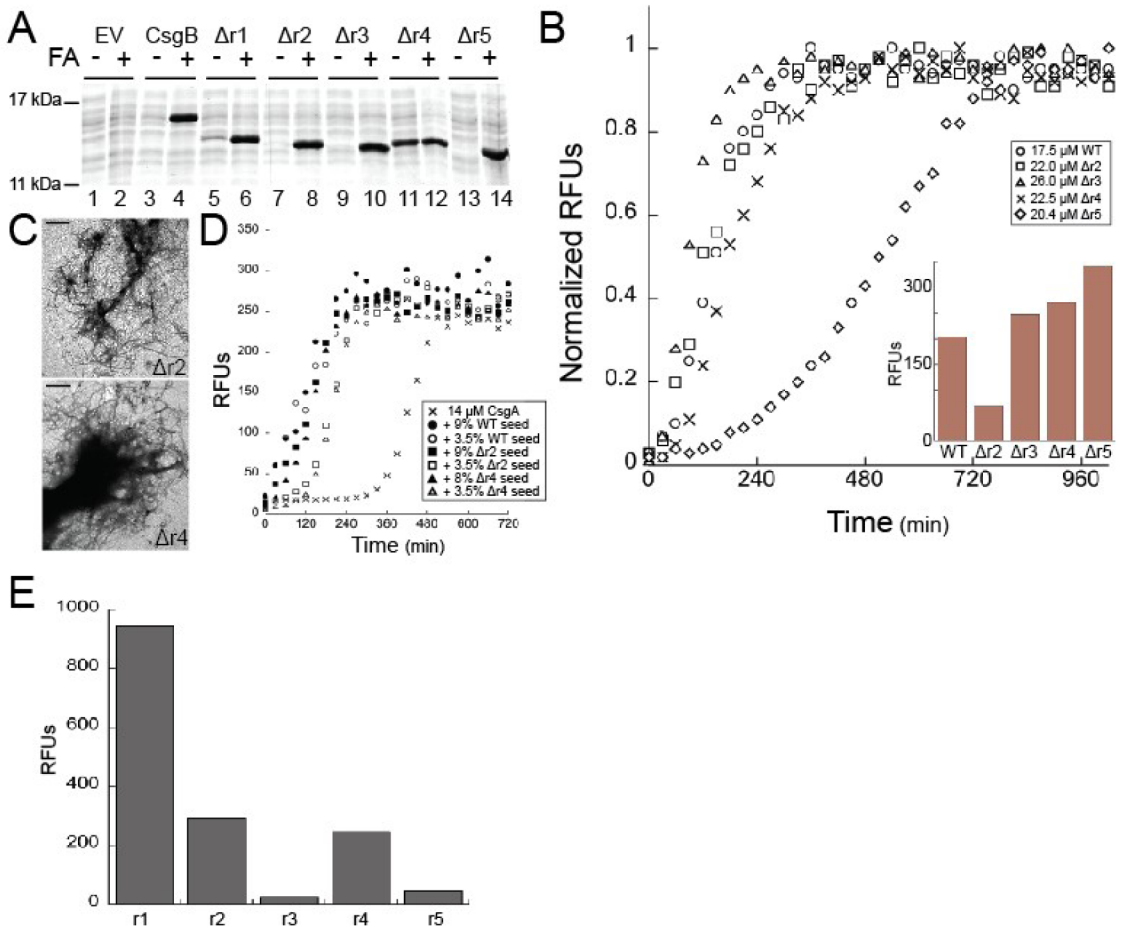

Figure 4. *In vitro* characterization of the repeating unit deletions

(A) Coomassie stained SDS-PAGE of OD_{600} normalized cell lysates of cells harboring the empty vector (EV) pET11d (EV lanes 1 and 2), WT CsgB (lanes 3 and 4), $CsgB^{\Delta r1}$ (Δr1 lanes 5 and 6), $CsgB^{\Delta r2}$ (Δr2 lanes 7 and 8), $CsgB^{\Delta r3}$ (Δr3 lanes 9 and 10), $CsgB^{\Delta r4}$ (Δr4 lanes 11 and 12), or $CsgB^{\Delta r5}$ (Δr5 lanes 13 and 14) after 1 hour induction with 0.5 mM IPTG. Samples were resuspended in SDS loading buffer with (+) or without (−) formic acid (FA) pretreatment. (B) Representative ThT kinetic plot of purified WT CsgB (○), $CsgB^{\Delta r2}$ (Δr2□), $CsgB^{\Delta r3}$ (Δr3△), $CsgB^{\Delta r4}$ (Δr4 X), and $CsgB^{\Delta r5}$ (Δr5 ◇). The inset is a representative bar graph of the RFUs for each protein after 12 hours of incubation at room temperature with ThT. (C) TEM of purified $CsgB^{\Delta r2}$ (Δr2 top panel) or purified $CsgB^{\Delta r4}$ (Δr4 bottom panel) after 24 hours of incubation at room temperature. The scale bars represent 500nm. (D) Representative ThT kinetic plot monitoring the polymerization of 14 μM CsgA (X), ^{14} μM seeded with 9% w/w WT CsgB (●), seeded with 3.5% w/w WT CsgB (○), seeded with 9% w/w $CsgB^{\Delta r2}$ (Δr2 ■), seeded with 3.5% w/w $CsgB^{\Delta r2}$ (Δr2 □), seeded with 8% w/w $CsgB^{\Delta r4}$ (Δr4 ▲), or seeded with 3.5% w/w $CsgB^{\Delta r4}$ (Δr4 △). (E) Relative fluorescent units (RFUs) produced by synthetic peptides composed of the amino acids in r1 (145 μM), r2 (102 μM), r3 (138 μM), r4 (176 μM), and r5 (167 μM) after incubation at room temperature for 24 hours in the presence of ThT.